13. R. Pecora, Ed., *Dynamic Light Scattering: Applications of Photon Correlation Spectroscopy* (Plenum, New York, 1985).
14. K. S. Schmitz, *An Introduction to Dynamic Light Scattering by Macromolecules* (Academic Press, New York, 1990).
15. J. M. Schurr and K. S. Schmitz, *Annu. Rev. Phys. Chem.* **37**, 271 (1986).
16. J. G. Elias and D. Eden, *Macromolecules* **14**, 410 (1981).
17. _____, *Biopolymers* **20**, 2369 (1981).
18. P. J. Hagerman, *ibid.*, p. 1503; *ibid.* **22**, 811 (1983).
19. N. C. Stellwagen, *ibid.* **20**, 399 (1981).
20. R. J. Lewis, R. Pecora, D. Eden, *Macromolecules* **19**, 134 (1981).
21. S. Diekmann *et al.*, *Biophys. Chem.* **15**, 263 (1982).
22. L. Wang, M. M. Garner, H. Yu, *Macromolecules*, in press.
23. F. Rondelez, in *Laser Scattering in Fluids and Macromolecular Solutions*, V. Degiorgio, Ed. (Plenum, New York, 1980).
24. H. Hervet, W. Urbach, F. Rondelez, *J. Chem. Phys.* **68**, 2725 (1978).
25. B. A. Scalettar, J. E. Hearst, M. P. Klein, *Macromolecules* **22**, 4550 (1989).
26. J. R. Williamson and S. G. Boxer, *Biochemistry* **28**, 2819 (1989).
27. M. M. Tirado and J. Garcia de la Torre, *J. Chem. Phys.* **71**, 2581 (1979); *ibid.* **73**, 1986 (1980).
28. M. M. Tirado, M. C. Lopez Martinez, J. Garcia de la Torre, *ibid.* **81**, 2047 (1984).
29. J. Garcia de la Toree *et al.*, *Biopolymers* **23**, 611 (1984).
30. M. Mandelkern *et al.*, *J. Mol. Biol.* **152**, 153 (1981).
31. R. M. Venable and R. W. Pastor, *Biopolymers* **27**, 1001 (1988).
32. S. S. Sorlie and R. Pecora, *Macromolecules* **21**, 1437 (1988); *ibid.* **23**, 487 (1990).
33. R. J. Lewis, thesis, Stanford University, Stanford, CA (1985).
34. _____, D. Eden, R. Pecora, *Macromolecules* **20**, 2579 (1987).
35. R. J. Lewis, S. A. Allison, D. Eden, R. Pecora, *J. Chem. Phys.* **89**, 2490 (1988).
36. J. Seils and R. Pecora, unpublished results.
37. S. W. Provencher, *Comput. Phys. Commun.* **27**, 213, 229 (1982).
38. S. E. Bott, thesis, Stanford University, Stanford, CA (1984).
39. P. J. Hagerman and B. H. Zimm, *Biopolymers* **20**, 1481 (1981).
40. T. Yoshizaki and H. Yamakawa, *J. Chem. Phys.* **81**, 982 (1984).
41. B. H. Zimm, *ibid.* **24**, 269 (1956).
42. H. Yamakawa, *Modern Theory of Polymer Solutions* (Harper and Row, New York, 1971).
43. R. Pecora, *J. Chem. Phys.* **40**, 1604 (1964); *ibid.* **48**, 4126 (1968); *ibid.* **49**, 1032 (1968).
44. H. Yamakawa and M. Fujii, *ibid.* **64**, 5222 (1976).
45. S. A. Allison, S. S. Sorlie, R. Pecora, *Macromolecules* **23**, 1110 (1990).
46. D. B. Roitman and B. H. Zimm, *J. Chem. Phys.* **81**, 6333 (1984); *ibid.*, p. 6348; D. B. Roitman, in *Rotational Dynamics of Small and Macromolecules*, Th. Dorfmüller and R. Pecora, Eds. (Springer, Heidelberg, 1987).
47. S. R. Argon and R. Pecora, *Macromolecules* **18**, 1868 (1985); S. R. Aragon, *ibid.* **20**, 370 (1987).
48. C. B. Post and B. H. Zimm, *Biopolymers* **21**, 2123 (1982); *ibid*, p. 2139.
49. A. A. Brian, H. L. Frisch, L. S. Lerman, *ibid.* **20**, 1305 (1981).
50. J. Widom and R. L. Baldwin, *ibid.* **22**, 1595 (1983); *ibid.*, p. 1621.
51. T. Hard and D. R. Kearns, *ibid.* **25**, 1519 (1986).
52. W. Fulmer, J. A. Benbasat, V. A. Bloomfield, *ibid.* **20**, 1147 (1981).
53. M. G. Fried and V. A. Bloomfield, *ibid.* **23**, 2141 (1984).
54. T. Nicolai and M. Mandel, *Macromolecules* **22**, 438 (1989); *ibid.*, p. 2348.
55. H. Tj. Goinga and R. Pecora, unpublished results.
56. S. F. Schulz *et al.*, *J. Chem. Phys.* **92**, 7087 (1990).
57. T. E. Strzelecka and R. L. Rill, *J. Am. Chem. Soc.* **109**, 4513 (1987); *Biopolymers* **30**, 57 (1990).
58. Supported by the National Science Foundation and by the NSF-MRL program through the Center for Materials Research at Stanford University. I wish to thank my past and present collaborators on this work. They are cited in the references.

Polymer-Polymer Phase Behavior

FRANK S. BATES

Different polymers can be combined into a single material in many ways, which can lead to a wide range of phase behaviors that directly influence the associated physical properties and ultimate applications. Four factors control polymer-polymer phase behavior: choice of monomers, molecular architecture, composition, and molecular size. Current theories and experiments that deal with the equilibrium thermodynamics and non-equilibrium dynamics of polymer mixtures are described in terms of these experimentally accessible parameters. Two representative molecular architectures, binary linear homopolymer mixtures and diblock copolymers, exhibiting macrophase separation and microphase segregation, respectively, are examined in some detail. Although these model systems are fairly well understood, a myriad of mixing scenarios, with both existing and unrealized materials applications, remain unexplored at a fundamental level.

MIXING, ALLOYING, AND BLENDING ARE FAMILIAR TERMS that describe the process of combining two or more elements, compounds, or molecular species into a single product. The associated mechanical, chemical, electrical, and various other properties are largely determined by the resulting phase behavior. For example, copper and zinc form a single solid phase known as brass that is mechanically superior to either constituent alone. Nonequilibrium microstructured phases in steel, produced by adding carbon and other elements to iron, can impart exceptional strength and hardness. Mixtures of oil and water that normally macroscopically phase separate can be finely dispersed by the addition of small amounts of surfactant, which can lead to gross changes in wetting and flow properties. All of these effects can be obtained with polymer-polymer mixtures, sometimes with the use of a single pair of monomeric building blocks. Such a diverse range of phase behaviors and the accompanying breadth of materials applications stem from the unparalleled range of molecular architectures that can be realized with polymers.

This article reviews polymer-polymer phase behavior beginning with a discussion of molecular architecture. Subsequently, overviews of equilibrium thermodynamics and phase separation dynamics are presented. Attention is restricted to binary combinations of amorphous polymers since most of the fundamental theoretical and experimental efforts have focused on these materials; crystalline polymers and multicomponent mixtures fall outside the scope of this article. The subject matter can be further subdivided into two categories, homopolymer mixtures and block copolymers. In each, discussion is focused on the most basic molecular architectures, that is, linear homopolymers and diblock copolymers, since these have been studied most intensely. A summary and brief comment regarding future prospects for this field are presented in the final section.

Molecular Architecture

The number of molecular configurations available to a pair of chemically distinct polymer species (here we define a polymer as a

The author is in the Department of Chemical Engineering and Materials Science, University of Minnesota, Minneapolis, MN 55455.

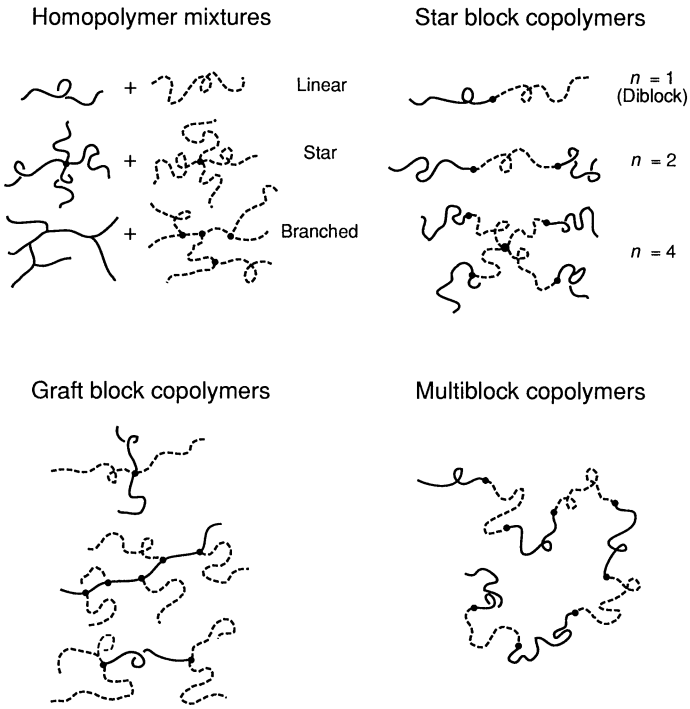

Fig. 1. Typical polymer-polymer (dashed and solid curves) molecular architectures attainable through the polymerization of two distinct monomers.

sequence of many repeat units) is almost unlimited. A small subset of the possibilities, representing four commonly encountered types of combinations, is illustrated in Fig. 1. The simplest and best understood among these is the case of binary homopolymer mixtures. At equilibrium such mixtures consist of either one or two phases (neglecting crystallization). In the event of phase separation, interfacial tension favors a reduction in surface area that leads to macroscopic segregation as sketched in Fig. 2A. However, polymer melts (materials that have been heated above the glass transition temperature T_g) are extremely viscous so that phase-separated homopolymers essentially never reach an equilibrium morphology (see the section below on phase-separation dynamics). Consequently, molecular architecture, which strongly influences polymer mobility, plays an important role in the evolution of phase morphology. Branching in particular disrupts the basic mechanism of polymer motion (*1*) (known as reptation) and leads to significant increases in viscosity. Since the majority of experimental and theoretical studies of homopolymer mixtures has been directed at linear macromolecules, the discussion is limited to this type of mixture. Nevertheless, the qualitative features identified are applicable to star and branched architectures provided the governing thermodynamic and dynamic relations are appropriately modified.

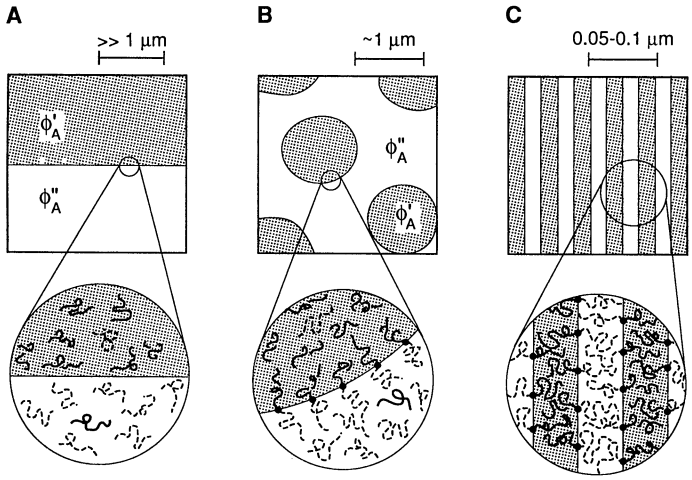

Fig. 2. (**A–C**) Representative polymer-polymer phase behaviors that can be realized with different molecular architectures. Macrophase separation (A) results when thermodynamically incompatible linear homopolymers are mixed. The covalent bond between blocks in a diblock copolymer leads to microphase segregation (C). A mixed architecture of linear homopolymers and the corresponding diblock copolymer produces a surfactant-like stabilized intermediate-scale phase separation (B).

Linear and star homopolymers with well-defined molecular weights and narrow molecular weight distributions are readily synthesized by using anionic polymerization techniques (*2, 3*). Alternative synthetic procedures (*4*), such as those used in the commercial production of linear and branched homopolymers, usually lead to less-ideal molecular structures that are not as attractive for model studies of polymer-polymer phase behavior.

Formation of block copolymers is an alternative method of mixing chemically different polymers. This seemingly minor chemical modification of covalently bonding polymer A to polymer B can be performed in inumerable ways, each with particular thermodynamic and dynamic consequences. Three classes of commonly encountered block copolymer architectures are identified in Fig. 1.

Star block copolymers represent the best defined group of block copolymers available at present. Model materials with specific arm number, composition, and molecular weight, and with a narrow molecular weight distribution can be prepared by anionic polymerization techniques (*2, 3*). These attributes have led many experimentalists and nearly all theoreticians to focus on this class of block copolymers; examples are discussed in the two sections below.

Graft and multiblock copolymers compensate with commercial importance what is lacking in architectural perfection. Synthetic routes to these materials generally lead to broad molecular weight distributions and variable graft and block functionalities. Graft block copolymers are frequently blended with homopolymers (see below), whereas multiblock copolymers, such as polyurethanes, are usually prepared neat.

In all cases the most significant factor in determining block-copolymer phase behavior is the covalent bond that restricts macroscopic separation of chemically dissimilar polymer blocks. This constraint leads to the formation of microscopic heterogeneities in composition at length scales comparable to the molecular dimensions, that is, around 50 to 1000 Å, which contrasts sharply with the macroscopic phase separation associated with binary mixtures. An example of such a microstructured (and ordered) phase is given in Fig. 2C for a symmetric (50% by volume component A) diblock copolymer. Such microphase segregation characterizes all block copolymers. However, detailed theoretical predictions for the associated phase behavior (such as the shape and packing symmetry of the microstructures) are only available for certain model star block copolymers, as described below.

Thus far specific molecular architectures have been considered individually. Many multicomponent polymer applications exploit mixed molecular architectures, such as combinations of graft block copolymers and homopolymer mixtures. In this case block copolymers can function as surfactants, localizing at interfaces in a two-phase system and thereby reduce the equilibrium phase size, as illustrated in Fig. 2B. Molecular architecture plays a significant role in delimiting the molecular weight, composition, and concentration of block copolymer required to obtain a particular particle size. Homopolymer architecture, molecular weight, and composition also contribute to the ultimate phase behavior. For example, if the molecular weight of homopolymer is significantly greater than that of diblock copolymer, a three-phase system (A-rich, B-rich, and

A-B–rich) can result rather than the surface-stabilized two-phase state depicted in Fig. 2B. Understanding of mixed architecture systems is rather limited, although recent progress can be found for diblock copolymer-linear homopolymer mixtures (*5, 6*). Notable examples of commercially important mixtures of graft block copolymers and linear homopolymers are high-impact polystyrene (HIPS) and acrylonitrile-butadiene-styrene (ABS) resins (7). Both materials derive superior impact strength from stabilized two-phase morphologies similar to that shown in Fig. 2B.

In the following sections macrophase separation and microphase segregation is examined in terms of the simplest and most studied molecular architecture in each category, binary linear homopolymer mixtures and diblock copolymers, respectively. Although the understanding of these model systems is rather well developed (*8, 9*), it should be recognized at the outset that the broader scope summarized by Fig. 1 (including mixed architectures) remains largely unexplored at a fundamental level.

Thermodynamic Parameters

Equilibrium polymer-polymer phase behavior is controlled by four factors: (i) molecular architecture (see previous section), (ii) choice of monomers, (iii) composition, and (iv) degree of polymerization. Composition generally refers to the overall volume fraction of a component. For homopolymer mixtures this parameter is frequently associated with the symbol ϕ, while recent custom assigns f to the star block–copolymer composition. Experimentally, ϕ is varied by simply changing the mixture stoichiometry. Shifting f requires the synthesis of a new material, since individual blocks are chemically bonded together. The degree of polymerization is the number of repeat units (monomers) that make up a polymer chain. Most thermodynamic theories presume a single repeat unit volume, although in practice chemically different repeat units rarely occupy equal volumes. Therefore, it is convenient to define a segment volume V corresponding to either of the repeat unit volumes (V_A or V_B), or any suitable mean repeat unit volume, for example, $V_A^{1/2} V_B^{1/2}$. With this definition the number of segments per polymer molecule is $N = \rho V \mathcal{N}/M$, where ρ and M are the polymer density and molecular weight, and $\mathcal{N}$ is Avogadro's number. Note that based on this convention $f = N_A/N$.

The choice of a particular pair of monomers establishes the sign and magnitude of the energy of mixing, which can be approximated by the Flory-Huggins segment-segment interaction parameter χ (*1, 10*),

$$\chi = \frac{1}{k_B T}\left[\epsilon_{AB} - \frac{1}{2}(\epsilon_{AA} + \epsilon_{BB})\right] \quad (1)$$

where ϵ_{ij} represents the contact energy between i and j segments, and k_B is the Boltzmann constant. A negative value of χ results from a favorable energy of mixing, that is, A–B segment-segment contacts on average produce a lower system energy than the sum of A–A and B–B contacts. Certain types of specific A–B interactions, such as hydrogen bonding, can result in a negative χ parameter. Positive values of χ occur when the net system energy increases upon forming A–B contact pairs from unmixed (pure) components. Most nonpolar polymers, such as polyethylene, polystyrene, and polyisoprene, are characterized by dispersive (van der Waals) interactions that can be represented by (*1*),

$$\epsilon_{ij} = -\sum_{i,j} \frac{3}{4} \frac{I_i I_j}{I_i + I_j} \frac{\alpha_i \alpha_j}{r_{ij}^6} \quad (2)$$

where r_{ij} is the segment-segment separation, and α and I are the segment polarizability and ionization potential, respectively. If there is no volume change ($\Delta V_m = 0$) or preferential segment orientation upon mixing, Eqs. 1 and 2 can be rearranged to

$$\chi = \frac{3}{16} \frac{I}{k_B T} \frac{z}{V^2} (\alpha_A - \alpha_B)^2 \quad (3)$$

where a cubic lattice is assumed with $I_j = I_j \equiv I$ (valid within 10% for most hydrocarbon polymers) and all but the z nearest-neighbor contacts are neglected. Thus, for polymer mixtures governed solely by dispersion interactions, $\chi \geq 0$.

In practice the assumptions made in deriving Eq. 3 are rarely realized. Significant deviations from incompressibility ($\Delta V_m \neq 0$) necessitate equation-of-state corrections to χ (*11–13*). Anisotropic monomer structures may lead to nonrandom segment packing that must be absorbed in χ as an excess entropy of mixing. These effects are usually accounted for by assuming that

$$\chi = \alpha T^{-1} + \beta \quad (4)$$

where α and β represent experimentally determined enthalpy and excess entropy coefficients for a particular composition. In general α and β may depend on ϕ (or f), N, T, and molecular architecture. Most molecular theories of polymer-polymer phase behavior have been developed by assuming a simple form for χ (such as Eq. 2). Nevertheless, application of these derivations usually requires the use of Eq. 4. Although this complication is ignored for the remainder of this article, the reader should recognize that specific interactions, preferential segment orientation, and equation-of-state effects play an important, albeit poorly understood, role in dictating phase behavior.

Phase state is governed by a balance between enthalpic ($H = U + PV$ where U, P, and V represent the system energy, pressure, and volume, respectively) and entropic (S) factors that together constitute the system (Gibbs) free energy (*10, 14*),

$$G = H - TS \quad (5)$$

Theoretical expressions for G are the starting point for predicting equilibrium phase behavior. Statistical models for the molecular configuration of a mixture that depend on molecular architecture, ϕ (or f), N, and χ are the basis for formulating the mixture free energy. Two representative cases, linear binary homopolymer mixtures and diblock copolymers, are examined below.

Linear Homopolymer Mixtures

Equilibrium phase behavior. Nearly 50 years ago Flory (*15*) and Huggins (*16*) independently estimated the change in free energy per segment ΔG_m associated with mixing random walk (Gaussian) polymer chains on an incompressible ($\phi_A + \phi_B = 1$) lattice,

$$\frac{\Delta G_m}{k_B T} = \frac{\phi_A}{N_A} \ln \phi_A + \frac{(1 - \phi_A)}{N_B} \ln(1 - \phi_A) + \phi_A(1 - \phi_A)\chi \quad (6)$$

The first two terms (right-hand side) account for the combinatorial entropy of mixing ΔS_m. Because mixing increases the systems randomness, it naturally increases ΔS_m and thereby decreases the free energy of mixing. Large chains can assume fewer mixed configurations than small chains so that ΔS_m decreases with increasing N. The third term represents the enthalpy of mixing ΔH_m and can either increase or decrease ΔG_m depending on the sign of χ (see above). Equation 6 is a mean-field theory that neglects spatial fluctuations in composition. For $N = 1$ it reduces to regular solution theory, which is widely applied to low molecular weight solution

thermodynamics (*14*).

The phase behavior can be predicted with Eq. 6 based on the standard criteria for equilibrium, the limits of stability, and criticality (*1,10*) evaluated at constant temperature and pressure:

$$\text{Equilibrium: } \frac{\partial \Delta G_m(\phi'_A)}{\partial \phi_A} = \frac{\partial \Delta G_m(\phi''_A)}{\partial \phi_A} \quad (7)$$

$$\text{Stability: } \frac{\partial^2 \Delta G_m}{\partial \phi_A^2} = 0 \quad (8)$$

$$\text{Criticality: } \frac{\partial^3 \Delta G_m}{\partial \phi_A^3} = 0 \quad (9)$$

where the superscripts ′ and ″ refer to separate phases. Plotted in Fig. 3 is the theoretical phase diagram for the symmetric case $N_A = N_B \equiv N$. The solid curve represents the solution of Eq. 7. For combinations of χN and ϕ lying inside this curve a mixture separates into two phases with compositions ϕ'_A and ϕ''_A. Between the solid and dashed curves a homogeneous mixture is thermodynamically metastable, while inside the dashed curve a mixture is thermodynamically unstable. The issues of metastability and stability are discussed in the section below on phase-separation dynamics. At the critical point the equilibrium and stability curves coincide. Combination of Eqs. 8 and 9 yields

$$\phi_c = \frac{N_A^{1/2}}{N_A^{1/2} + N_B^{1/2}} \quad (10)$$

and

$$\chi_c = \frac{(N_A^{1/2} + N_B^{1/2})^2}{2N_A N_B} \quad (11)$$

where the subscript c signifies criticality. For a symmetric mixture $(\chi N)_c = 2$ and $\phi_c = 0.5$, as indicated in Fig. 3.

These calculations illustrate two distinctive features of homopolymer phase behavior. Once a particular monomer pair is chosen, thus fixing $\chi = f(T)$, the critical temperature T_c can be varied by adjusting N (Eq. 11). Also, the critical composition can be controlled by manipulating the ratio N_A/N_B (Eq. 10). In this way phase diagrams can often be tailored to accommodate experimental constraints, such as glass-transition or thermal-decomposition temperatures. The extent to which this is possible depends on the temperature, composition, and molecular weight dependence of χ (see above). For example, if α is positive and β is negative in Eq. 4, decreasing temperature always increases χ and an upper critical solution temperature (UCST) results (that is, the two-phase envelope is concave down in the coordinates ϕ versus T). If α is negative and β positive, then a lower critical solution temperature (LCST) may result (that is, the two-phase envelope is concave up in ϕ versus T) depending on the magnitude of N and β. More complex functional forms for χ can produce both UCST and LCST behavior (*11–13*).

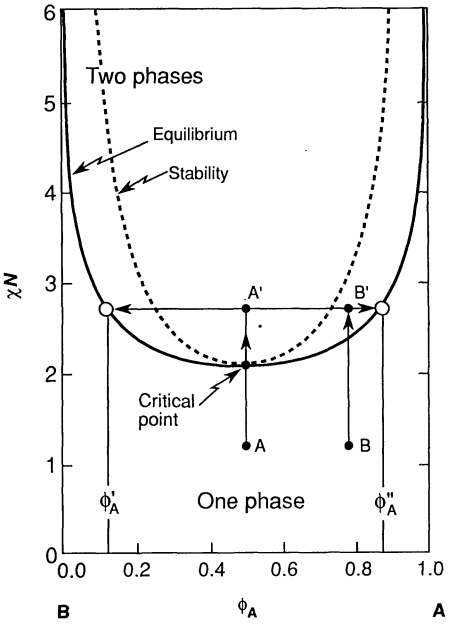

Fig. 3. Theoretical phase diagram (mean field) for a symmetric ($N_1 = N_2 \equiv N$) binary mixture of linear homopolymers; [N, ϕ_A and $\chi(T)$ are the polymer degree of polymerization, volume fraction of component A, and segment-segment interaction parameter, respectively (see Eqs. 6 to 9)]. Inside the equilibrium (solid) curve, two phases exist with compositions ϕ'_A and ϕ''_A. In the metastable region (such as point B′), phase separation occurs by a nucleation and growth mechanism, while an unstable mixture (such as point A′) spontaneously demixes by spinodal decomposition (see Fig. 4).

In spite of the need to treat χ as a largely phenomenalogical parameter, homopolymer mixtures are in many respects more ideal and better applied to fundamental studies of phase behavior than their low molecular weight counterparts. Unlike the latter, this class of mixtures is well described by mean-field theory (such as Eq. 6) over all but a miniscule region of phase space around the critical point (see Fig. 3). This characteristic can be traced to the large dimensions associated with polymer chains. One useful measure of polymer size is the radius-of-gyration, $R_g = a(N/6)^{1/2}$, where a represents the length of a segment (*1, 10*). For polystyrene, $a = 6.8$ Å, which leads to $R_g = 270$ Å for a sample with a molecular weight of 10^6 (*17*). In this case a single molecular volume, approximated as $(4/3)\pi R_g^3$, contains 50 other polystyrene chains, which virtually assures average (mean-field) segment-segment interactions except where composition fluctuations become much longer ranged than R_g. Since the mean-field composition fluctuation length ξ scales as (*1*) $\xi \sim (\chi_c - \chi)^{-1/2}$, the condition for crossover from mean-field to non–mean-field behavior ($\xi \sim R_g$), known as the Ginzburg criterion (*18*) scales as $|\chi_c - \chi| \sim N^{-1}$. Thus, increasing N shrinks the non–mean-field region to a small area around the critical point. In contrast, for monomers ($N = 1$) composition fluctuations influence the entire phase diagram.

Fluctuation effects are important in many areas of materials science and condensed-matter physics (*19*), including magnetism, superconductivity, and liquid crystallinity. However, the ability to influence the Ginzburg criterion through the choice of monomers and N makes polymer mixtures attractive for investigating the limitations of mean-field theory. Recent studies of critical mixtures of poly(vinyl methyl ether) and polystyrene (LCST) (*20*), and poly(ethylene-propylene) and polyisoprene (UCST) (*21*) underscore this point in providing the first quantitative verification of the Ginzburg criterion.

Since $\chi_c \sim N^{-1}$ (Eq. 11), homopolymer phase behavior can be influenced by remarkably subtle chemical or structural variations between components. A dramatic demonstration of this point is provided by mixtures of deuterated and normal (protonated) polymers that are otherwise chemically indistinguishable. Until recently such isotopic mixtures were generally assumed to form ideal solutions ($\chi = 0$). However, several years ago it was discovered that above a molecular weight of $\sim 1.8 \times 10^5$ g/mol symmetric mixtures of deuterated and protonated polybutadienes phase separate (*22*). This phenomenon has since been shown to be universal and predictable (*23*). It derives from the well-known reduction in carbon-hydrogen bond length (~0.1%) that accompanies deuterium substitution in organic molecules. Decreasing the bond length reduces the bond polarizability, which is manifested as a decreased segment polarizability. Together these two effects produce a small positive χ parameter, as predicted by Eq. 3.

The polymer isotope effect is an extremely valuable tool for investigating the thermodynamics and dynamics of polymer-polymer mixing and demixing. Because polymer isotopes are chemically identical, they very nearly satisfy the assumptions underlying most statistical mechanical theories of polymer thermodynamics, which is that the repeat units are structurally symmetric. This fact is reflected in the ability of Eq. 3 to predict the magnitude of χ based on independent estimates of α and V (*23*). Recent experiments with isotopic polymer mixtures (*24*) have for the first time identified deficiencies in the Flory-Huggins combinatorial entropy of mixing; prior studies could not discriminate between this effect and various other empirical corrections to χ (see above). Other current applications include studies of wetting (*25*), interfacial mixing (*26*), and phase-separation dynamics (*27*).

Significant advances in the theoretical treatment of binary polymer mixtures have also been achieved in the past few years. Freed and co-workers (*28, 29*) have addressed the issues of structural asymmetry by incorporating a variable monomer structure (such as pendent groups with different sizes and degrees of branching) into an improved lattice theory. This refinement produces a rich concentration dependence to χ that varies with the magnitude of ϵ_{ij} (Eq. 2). In an alternative approach, Curro and Schweizer (*30, 31*) report the application of modern liquid-state theory, developed over the past two decades for simple fluids, to the problem of polymer-polymer mixtures. This approach couples conventional long-range polymer-coil statistics with the short-range constraints imposed by local liquid structure. They also predict a composition dependent χ along with a nonclassical scaling behavior for the critical point; for a symmetric mixture they find $\chi_c \sim N^{-1/2}$, in contrast with the Flory-Huggins prediction (Eq. 11) that $\chi_c \sim N^{-1}$. Verification of these newly developed theories represents an important experimental challenge.

Phase-separation dynamics. Homopolymer mixtures in the one-phase region of the phase diagram are easily homogenized by mechanical mixing or solution casting. Noryl, a commercial plastic composed of poly(phenylene oxide) and polystyrene, is an example of such a homogeneous alloy (*32*). Conversely, equilibrium is neither desirable nor practically attainable with two-phase polymer mixtures. Homopolymer phase behavior can be accurately represented by mean-field theory. Therefore, phase-separation dynamics can be divided into two categories, nucleation and growth and spinodal decomposition, as illustrated in Fig. 3.

Classical nucleation theory (*34, 34*) predicts that small droplets of a minority phase develop over time in a homogeneous mixture that has been brought into the metastable region of the phase diagram (for example, from point B to B′ in Fig. 3). Initially droplet growth proceeds by diffusion of material from the supersaturated continuum. However, once the composition of the supernatant reaches equilibrium (ϕ''_A in Fig. 3), further increases in droplet size occur by droplet coalescence or Ostwald ripening; the latter refers to the growth of large droplets through the disappearance ("evaporation") of smaller ones. Because of the extremely low diffusivity ($D \sim N^{-2}$) and enormous viscosity ($\eta \sim N^{3.4}$) of polymers (*1*), the second stage of growth can be extremely slow and may result in unusual particle-size distributions (*35*).

In the metastable state, homogeneous mixtures must overcome a free energy barrier in order to nucleate a new phase. In the thermodynamically unstable state there is no such barrier, and mixtures phase separate spontaneously (for example, from point A to A′ in Fig. 3). This process, which was first described theoretically by Cahn 25 years ago (*36*), is known as spinodal decomposition. It results in a disordered bicontinuous two-phase structure that is contrasted in Fig. 4 with the morphology associated with the nucleation and growth mechanism. The initial size d_0 of the spinodal structure (see Fig. 4) is controlled by the quench depth $\chi_s - \chi$, where χ_s corresponds to the stability limit (dashed curve in Fig. 3); deeper quenches produce finer structures. Almost immediately after the bicontinuous pattern begins to form, interfacial tension drives the system to reduce its surface area by increasing d. In symmetric critical mixtures ($N_A = N_B \equiv N$ and $\phi_c = 1/2$) coarsening does not disrupt the bicontinuous morphology that evolves through a universal, scale invariant form, as depicted in Fig. 4.

The intricate structures associated with spinodal decomposition lead to a variety of interesting materials applications. These include polymer-based membranes (*37*), controlled porous glasses (*38*), and certain metal and ceramic alloys (*39*). Linear homopolymer mixtures have become one of the most attractive systems for studying spinodal decomposition in recent years (*27, 40*). Applicability of mean-field theory simplifies the theoretical analysis considerably. However, the greatest advantages are a tunable phase diagram (see Eqs. 10 and 11) and an extremely low rate of phase separation. Under comparable conditions spinodal decomposition in polymer mixtures is $\sim N^2$ slower than in low molecular weight mixtures (*27, 41*). A recent study of spinodal decomposition in nearly symmetric polybutadiene isotopes (*27*) illustrates these points. Selection of $N = 3 \times 10^4$ for this pair of isotopes resulted in a UCST at 61°C. Following a quench from 75° to 25°C (this is analagous to A to A′ in Fig. 3), an initial spinodal pattern with $d \cong 0.23$ μm developed within 30 min. The structure required 24 hours to coarsen to 1 μm, and 2 months passed before a period of 5 μm was realized. In contrast, in most monomeric mixtures this entire process would take only several seconds. By telescoping the time scale for spinodal decomposition, the evolving composition patterns can be examined in greater detail through the use of scattering (light and neutrons) and microscopy techniques (*27*). The results of these studies are enhancing our general understanding of phase-separation dynamics.

Diblock Copolymers

Order and disorder. The ensemble of molecular configurations that produces the minimum overall free energy G represents the equi-

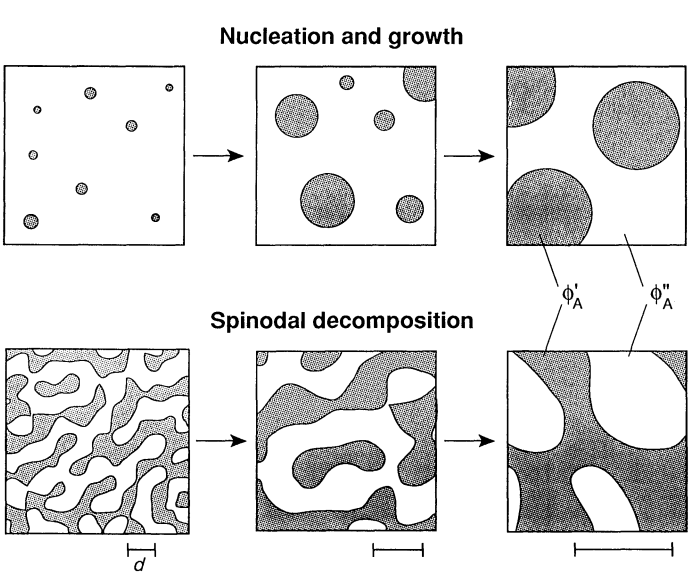

Fig. 4. Time evolution of structure in phase-separating binary homopolymer mixtures. Nucleation and growth results when a homogeneous mixture is thrust into the metastable region of the phase diagram (such as B → B′ in Fig. 3). Spinodal decomposition occurs when a mixture is placed in a thermodynamically unstable state (such as A → A′ in Fig. 3). The driving force behind coarsening in both cases is the minimization of interfacial tension through a reduction in interfacial area.

librium state in a block copolymer melt (*42–45*). Note that this criterion differs from the condition for equilibrium in homopolymer mixtures (Eq. 7) because block copolymers are single component systems that cannot phase separate. When $\chi > 0$ a decrease in *A–B* segment-segment contacts in an *A–B* diblock copolymer reduces the system enthalpy *H*. This process can occur locally, segregating *A* and *B* blocks (Fig. 2C). Segregation is opposed by the associated loss in system entropy that derives from (i) localizing block-block joints at interfaces and (ii) stretching the chains in order to maintain a uniform density (stretching a polymer chain reduces its configurational entropy). Diblock copolymer entropy also scales as $S \sim N^{-1}$, and as before it is the product χN that controls the state of segregation (*9*). However, the nature of block segregation is quite different from phase separation that occurs with homopolymers.

For $\chi N << 10$, entropic factors dominate and diblock copolymers exist in a spatially homogeneous state (*43*). Increasing *N* or χ shifts the free energy balance and leads to the development of local composition fluctuations (*45*) on a scale proportional to the polymer radius-of-gyration ($R_g^2 = R_{g,A}^2 + R_{g,B}^2$), as depicted in Fig. 5. When $\chi N \approx 10$, a delicate balance exists between entropic and energetic effects. Increasing this parameter further induces a first-order transition to an ordered state (*43, 45*). In this case entropically favored but energetically costly curved and disordered microstructures are exchanged for a periodic mesophase. This phase transition, known as the order-disorder transition (ODT), resembles the familiar freezing transition in low molecular weight systems, such as water at 0°C. Increasing χN still further leads to sharper microdomain boundaries as the number of *A–B* segment-segment contacts decrease at the expense of additional chain stretching. In the limit $\chi N >> 10$, energetic factors dominate and the ordered microstructures are characterized by narrow interfaces and nearly flat composition profiles (*42, 44*) (see Fig. 5).

Thus far we have only considered the symmetric case $f = 1/2$ (see Figs. 2C and 5). Changes in *f* primarily affect the shape and packing symmetry of the ordered microstructure and, except near the ODT (see below), are almost uncorrelated with χN (*42, 44*). Reducing or increasing *f* places unequal packing and chain stretching constraints on each side of a diblock copolymer molecule and leads to new ordered-phase symmetries over specific ranges in composition. Seven ordered phases have been identified in the polystyrene-polyisoprene (PS-PI) system, as illustrated in Fig. 6A, where f_s denotes the volume fraction of polystyrene (*46, 47*).

For $f_s < 0.17$, microspheres of polystyrene are ordered on a body-centered cubic (bcc) lattice in a matrix of polyisoprene. Increasing the composition to $0.17 < f_s < 0.28$ leads to hexagonally packed (hex) cylindrical microdomains. An ordered bicontinuous double diamond (obdd) polystyrene microstructure embedded in a continuous polyisoprene microphase appears where $0.28 < f < 0.34$. This most recent addition to the family of documented equilibrium ordered phases in PS-PI is particularly interesting since it contains a triply periodic constant mean curvature (CMC) surface (*48*). Because variations in surface area and curvature directly influence the ordered-state free energy, block copolymers can provide a physical manifestation of abstract mathematical concepts used to describe CMCs (*49*). Between $f_s = 0.34$ and 0.62 these materials display a lamellar microstructure. Increasing f_s further leads to the corresponding inverted ordered phases (Fig. 6A). Combining the effects of varying χN and *f* results in the PS-PI diblock copolymer phase diagram shown in Fig. 6B.

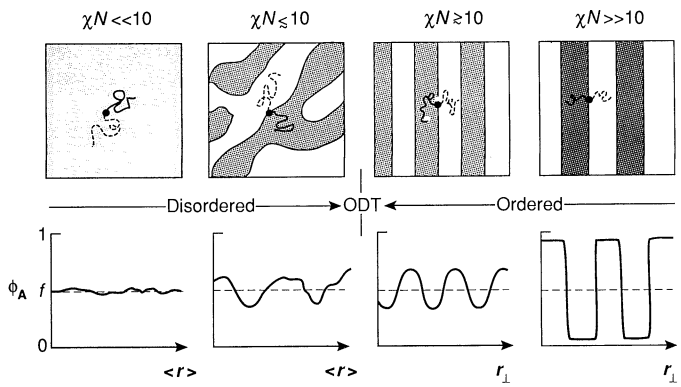

Fig. 5. Evolution of structure with the combined parameter χN for a symmetric, diblock copolymer with $f = 0.5$. When $\chi N \sim 10$, small variations in system entropy ($\sim N^{-1}$) or energy ($\sim \chi$) leads to ordered ($\chi N \gtrsim 10$) or disordered ($\chi N \lesssim 10$) states. A homogeneous composition profile (ϕ_A versus *r*) results when entropic factors dominate ($\chi N << 10$), whereas a strongly microphase segregated pattern characterizes the limit where energetic factors prevail ($\chi N >> 10$).

Theories that deal with block-copolymer phase behavior can be divided into two categories: (i) strong segregation limit (*42, 44*) (SSL, $\chi N >> 10$) and (ii) weak segregation limit (*43, 45*) (WSL, $\chi N \lesssim 10$). In the SSL theories well-developed microdomain structures are assumed to occur with relatively sharp interfaces and chain stretching is explicitly accounted for. The WSL theories are premised on lower amplitude sinusoidal composition profiles and unperturbed Gaussian coils, that is, they neglect chain stretching (see Fig. 5). Mean-field SSL theories are reasonably successful at predicting how microdomain symmetry, size, and periodicity depend on *N*, *f*, and χ away from the ODT, although to date the existence of an obdd phase has not been accounted for (*50*).

Near the ODT the situation is more complex. Here the delicate balance between χ and *N* can be influenced by *f* and can lead to curvature in the order-order transition lines. Composition fluctuations, which are insignificant when $\chi N << 10$ and $\chi N >> 10$ (see Fig. 5), can undermine the use of mean-field theory and further complicate the analysis. Recent theoretical (*45*) and experimental (*51, 52*) progress in this area has demonstrated that these effects lead to non-universal phase behavior, that is, a unique phase diagram can be associated with each value of *N*. However, WSL fluctuation theory fails to account for polymer chain stretching near the ODT, which has been documented experimentally (*53*).

Recent experiments (*54*) on an $f = 0.65$ poly(ethylene-propylene)–poly(ethylethylene) (PEP-PEE) diblock copolymer have revealed three distinct ordered phases, along with a disordered phase, that can be accessed by varying temperature. This discovery lends support to the notion of a non-universal diblock-copolymer phase diagram; note that more than two decades of intense study of the PS-PI system has yet to uncover any order-order transitions controlled by temperature alone. The increase in phase complexity in PEP-PEE polymers may be attributable to a smaller χ parameter (approximately one-fifth that of PS-PI). Decreasing χ, which necessitates increasing *N* in order to maintain an experimentally viable ODT temperature, necessarily increases the sensitivity of a block copolymer system to minor perturbations in free energy, whether energetic or entropic in origin. As a consequence, small variations in interfacial structure or chain stretching might be balanced by minimizing interfacial curvature or spatial variations in microdomain dimensions through transitions between nearly degenerate phases. Hence, block copolymer melts may represent ideal substrates for investigating the concept of periodic surfaces of prescribed mean curvature (*48*).

Long-range order. At equilibrium an ordered block copolymer will be macroscopically oriented, analogous to a single crystal of low molecular weight material. However, when quenched below the ODT an undisturbed disordered melt will rapidly order [except very close to the ODT (*51, 52*)] without a preferred direction. This

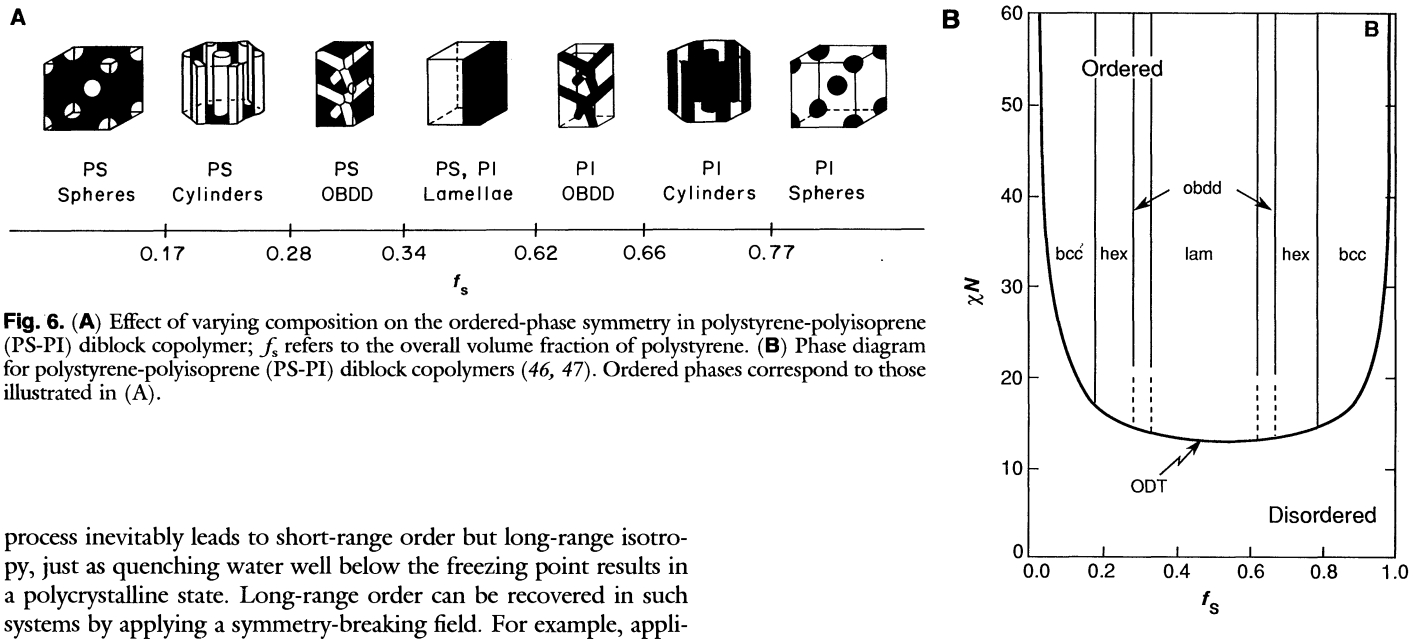

Fig. 6. (**A**) Effect of varying composition on the ordered-phase symmetry in polystyrene-polyisoprene (PS-PI) diblock copolymer; f_s refers to the overall volume fraction of polystyrene. (**B**) Phase diagram for polystyrene-polyisoprene (PS-PI) diblock copolymers (*46, 47*). Ordered phases correspond to those illustrated in (A).

process inevitably leads to short-range order but long-range isotropy, just as quenching water well below the freezing point results in a polycrystalline state. Long-range order can be recovered in such systems by applying a symmetry-breaking field. For example, application of a magnetic field to a ferromagnetic material as it is cooled below the Curie temperature induces a permanent net magnetic moment. Thermal gradients are used to prepare large single crystals of silicon by directional solidification, and an electric field can produce a high degree of orientation in liquid crystalline materials.

Ordered block copolymers respond to mechanical deformation. The application of a large-amplitude oscillatory shear field can convert a quenched (polycrystalline) specimen with $f \approx 0.5$ into a set of highly oriented lamellae (*55*); in this case the lamellae lie parallel to the plane of shear. Cylindrical microstructures also respond to a shear field, resulting in hexagonal single crystals (*56*). Such highly oriented materials are useful for studying the equilibrium state, particularly when multiple ordered phases are possible.

Long-range–ordered block copolymers also exhibit highly anisotropic properties. Because polystyrene is a glass and polyisoprene is rubbery at room temperature, an oriented PS-PI material containing polystyrene cylinders will be rubbery and glassy-like along directions perpendicular and parallel, respectively, to the microdomain long axis (see Fig. 6A). Highly oriented lamellae will also be characterized by anisotropic properties, such as gas permeability. At present, long-range order in block copolymers remains largely a laboratory curiosity. Nevertheless, the ability to control the size, spacing, and materials that constitute highly oriented microstructures such as those illustrated in Fig. 6A should result in creative applications.

Summary

Polymer-polymer phase behavior is a complex interdisciplinary subject that makes contact with numerous basic scientific concepts while also finding innumerable engineering applications. By controlling molecular architecture through synthetic chemistry a single pair of monomers can be directed into a wide variety of multiphase structures that vary dramatically in scale, form, and degree of order. The extremely long molecular relaxation times associated with undiluted high molecular weight polymers can be exploited to probe the fundamental principles of phase separation (such as spinodal decomposition) or ordering dynamics or can be applied toward optimizing physical properties such as toughness.

In this brief overview an attempt has been made to identify the basic factors that govern polymer-polymer phase behavior by focusing on two representative model molecular architectures. Both linear homopolymer mixtures and diblock copolymers have been subjected to intense study for many years. Nevertheless, the understanding of these most basic of molecular configurations continues to evolve, and this knowledge continues to have a significance impact on science and technology. Furthermore, this subject matter, which draws upon a host of traditional scientific and engineering disciplines, has only begun to be explored. More complex phase behaviors brought about by new molecular architectures, or mixtures of those presently available, should provide enticing challenges and opportunities well into the next century.

REFERENCES AND NOTES

1. P.-G. deGennes, *Scaling Concepts in Polymer Physics* (Cornell Univ. Press, Ithaca, NY, 1979).
2. J. E. McGarth, Ed., *Anionic Polymerization*, no. 166 of the *ACS Symposium Series* (American Chemical Society, Washington, DC, 1981).
3. M. Szwarc, *Advances in Polymer Science* (Springer-Verlag, New York, 1983), vol. 49.
4. G. Odian, *Principles of Polymerization* (Wiley-Interscience, New York, 1981).
5. T. Hashimoto, H. Tanaka, H. Hasegawa, *Macromolecules* **23**, 4378 (1990).
6. M. D. Whitmore and J. Noolandi, *ibid.* **18**, 2486 (1985).
7. N. G. McCrum, C. P. Buckley, C. B. Bucknall, *Principles of Polymer Engineering* (Oxford Univ. Press, New York, 1988).
8. O. Olabisi, L. M. Robeson, M. T. Shaw, *Polymer-Polymer Miscibility* (Academic Press, New York, 1979).
9. F. S. Bates and G. H. Fredrickson, *Annu. Rev. Phys. Chem.* **41**, 525 (1990).
10. P. J. Flory, *Principles of Polymer Chemistry* (Cornell Univ. Press, Ithaca, NY, 1953).
11. I. C. Sanchez, in *Polymer Blends*, D. R. Paul and S. Newman, Eds. (Academic Press, New York, 1978), vol. 1, pp. 115–139.
12. P. J. Flory, *J. Am. Chem. Soc.* **87**, 1833 (1965).
13. L. P. McMaster, *Macromolecules* **6**, 760 (1973).
14. E. A. Guggenheim, *Thermodynamics* (Elsevier, New York, 1985).
15. P. J. Flory, *J. Chem. Phys.* **10**, 51 (1942).
16. M. Huggins, *J. Phys. Chem.* **46**, 151 (1942); *J. Am. Chem. Soc.* **64**, 1712 (1942).
17. G. D. Wignall, in *Encyclopedia of Polymer Science and Engineering*, (Wiley, New York, 1987), vol. 10, pp. 112–184.
18. V. L. Ginzburg, *Sov. Phys. Solid State* **2**, 1824 (1960); K. Binder, *Phys. Rev. A* **29**, 341 (1984).
19. S.-K. Ma, *Modern Theory of Critical Phenomena*, vol. 46 of *Frontiers in Physics* (Benjamin, Reading, MA, 1976).
20. D. Schwahn, K. Mortensen, Y. Yee-Madeira, *Phys. Rev. Lett.* **58**, 1544 (1987).
21. F. S. Bates *et al.*, *ibid.* **65**, 1893 (1990).
22. F. S. Bates, G. D. Wignall, W. C. Koehler, *ibid.* **55**, 2425 (1985).
23. F. S. Bates, L. J. Fetters, G. D. Wignall, *Macromolecules* **21**, 1086 (1988).
24. F. S. Bates, M. Muthukumar, G. D. Wignall, L. J. Fetters, *J. Chem. Phys.* **89**, 535 (1988).
25. R. A. Jones, E. J. Kramer, M. H. Rafailovich, J. Sokolov, S. A. Schwarz, *Phys. Rev. Lett.* **62**, 280 (1989).
26. V. Steiner, G. Krausch, G. Schatz, J. Klein, *ibid.* **64**, 1119 (1990).

27. F. S. Bates and P. Wiltzius, *J. Chem. Phys.* **91**, 3258 (1989).
28. K. F. Freed and M. G. Bawendi, *J. Phys. Chem.* **93**, 2194 (1989).
29. J. Dudowicz, K. F. Freed, W. G. Madden, *Macromolecules* **23**, 4803 (1990).
30. K. S. Schweizer and J. G. Curro, *J. Chem. Phys.* **91**, 5059 (1989).
31. J. G. Curro and K. S. Schweizer, *Macromolecules* **23**, 1402 (1990).
32. W. J. MacKnight, F. E. Karasz, J. R. Fried, in *Polymer Blends*, D. R. Paul and S. Newman, Eds. (Academic Press, New York, 1978), vol. 1, pp. 185–242.
33. K. Binder, *J. Chem. Phys.* **79**, 6387 (1983).
34. F. F. Abraham, *Homogeneous Nucleation Theory* (Academic, New York, 1974).
35. A. Cumming, P. Wiltzius, F. S. Bates, *Phys. Rev. Lett.* **65**, 863 (1990).
36. J. W. Cahn, *J. Chem. Phys.* **42**, 93 (1965).
37. R. E. Kesting, *Synthetic Polymeric Membranes* (Wiley, New York, 1985).
38. P. Wiltzius, F. S. Bates, S. B. Dierker, G. D. Wignall, *Phys. Rev. A* **36**, 2991 (1987).
39. B. D. Gaulin, S. Spooner, Y. Morii, *Phys. Rev. Lett.* **59**, 668 (1987).
40. T. Hashimoto, M. Ikakura, H. Hasegawa, *J. Chem. Phys.* **85**, 6118 (1986); T. Hashimoto, M. Itakura, N. Shimidzu *ibid.*, p. 6773.
41. P. Guenon, R. Gastaud, F. Perrot, D. Beysens, *Phys. Rev. A* **36**, 4876 (1987).
42. E. Helfand and Z. R. Wasserman, in *Developments in Block and Graft Copolymers-1*, I. Goodman, Ed. (Applied Science, New York, 1982), pp. 99–125.
43. L. Leibler, *Macromolecules* **13**, 1602 (1980).
44. A. N. Seminov, *Sov. Phys. JETP* **61**, 733 (1985).
45. G. H. Fredrickson and E. Helfand, *J. Chem. Phys.* **87**, 697 (1987).
46. H. Hasegawa, H. Tanaka, K. Yamasaki, T. Hashimoto, *Macromolecules* **20**, 1641 (1987).
47. D. S. Herman, D. J. Kinning, E. L. Thomas, L. J. Fetters, *ibid.*, p. 2940.
48. D. M. Anderson, H. T. Davis, L. E. Scriven, J. C. C. Nitsche, *Adv. Chem. Phys.* 77, 337 (1990).
49. E. L. Thomas, D. M. Anderson, C. S. Henkel, D. Hoffman, *Nature* **334**, 598 (1988).
50. D. M. Anderson and E. L. Thomas, *Macromolecules* **21**, 3221 (1988).
51. F. S. Bates, J. H. Rosedale, G. H. Fredrickson, *J. Chem. Phys.* **92**, 6255 (1990); F. S. Bates, J. H. Rosedale, G. H. Fredrickson, C. J. Glinka, *Phys. Rev. Lett.* **61**, 2229 (1988).
52. J. H. Rosedale and F. S. Bates, *Macromolecules* **23**, 2329 (1990).
53. K. Almdal, J. H. Rosedale, F. S. Bates, G. D. Wignall, G. H. Fredrickson, *Phys. Rev. Lett.* **65**, 1112 (1990).
54. K. Almdal, K. Koppi, F. S. Bates, K. Mortensen, unpublished results.
55. G. Hadziioannou and A. Skoulios, *Macromolecules* **15**, 258 (1982).
56. A. Mathis, G. Hadziioannou, A. Skoulios, *Colloid Polym. Sci.* **257**, 136 (1979).
57. Support for this research was provided by the Air Force Office of Scientific Research, and the National Science Foundation through a Presidential Young Investigator (PYI) award (DMR-8957386) and the Center for Interfacial Engineering (CIE), an engineering research center at the University of Minnesota.

Polymer Brushes

S. T. MILNER

Polymers attached by one end to an interface at relatively high coverage stretch away from the interface to avoid overlapping, forming a polymer "brush." This simple picture may serve as the basis for models in diverse interfacial systems in polymer science, such as polymeric surfactants, stabilized suspensions of colloidal particles, and structures formed by block copolymers. The structure and dynamics of polymer brushes have been the subject of considerable theoretical and experimental activity in recent years. An account is given of recent advances in theoretical understanding of stretched polymers at interfaces, and the diverse experimental probes of systems modeled by brushes are briefly reviewed.

POLYMER "BRUSHES" ARE LONG-CHAIN POLYMER MOLECULES attached by one end to a surface or interface by some means, with a density of attachment points high enough so that the chains are obliged to stretch away from the interface, sometimes much farther than the typical unstretched size of a chain. This situation, in which polymer chains stretch along the direction normal to the grafting surface (like the bristles in a brush, hence the name), is quite different from the typical behavior of flexible polymer chains in a solution, where the long molecules adopt random-walk configurations.

Polymer brushes, with some important variations, are a central model in many important problems in polymer science, and are relevant even in biophysics and surfactant science (where the chains in question are only marginally long enough to be called polymers). One of the most important variations among brushes is the presence or absence of solvent for the polymer chains. With solvent present, the physical reason for the chains stretching away from the interface to which they are attached is their affinity for the solvent (and/or dislike of each other). For melt conditions (no solvent present), the chains must stretch away from the interface to avoid overfilling space (since the matter of which the chains are made is approximately incompressible).

The interface to which the chains in the brush are attached may be a solid substrate or the interface between two solvents, between solvent and air, or between melts or solutions of homopolymers. The mechanism by which the chains are attached to the interface varies with the interface. For solid substrates, the chain end may be chemically bonded to the substrate or the chain may be terminated by a special chemical group that adsorbs onto the surface. This end group may be either a small molecule that is strongly attracted to the surface, or a long copolymer, each monomer of which is only weakly attracted. For interfaces between fluids, the attachment may be achieved by similar adsorption mechanisms in which the end group of the chain prefers one medium and the chain prefers the other. Finally, the chain may be attached to a "substrate" that is the narrow interface between microdomains in a melt or concentrated solution of diblock copolymers (two dissimilar polymers joined end to end) when the two blocks of the copolymer are strongly segregated.

Within these variations in interface and solvents, several important physical systems are contained (see Fig. 1):

1) Colloid stabilization by end-grafted chains. In this case solid particles are maintained in suspension (protected against flocculation due to van der Waals attraction) by attaching a "brush" of grafted chains that prefer the solvent of the suspension; the brushes of two approaching particles resist overlapping, separating the particles to a distance at which the van der Waals interaction is too weak to keep the particles together.

2) Polymeric surfactants. A polar end-group is attached to a hydrocarbon chain, which is insoluble in polar solvents; a polymeric surfactant molecule is formed that is attracted to oil-water interfaces.

The author is in the Corporate Research Science Laboratories, Exxon Research and Engineering Company, Annandale, NJ 08801.